structural colors, that the color changes with viewing angle, is reproduced.

In thin-film interference, we usually consider only single reflections at each interface. However, with increasing reflectivity at an interface, multiple reflections should be important. The rigorous reflectivity in amplitude is given by Equation (2):

$$r = r_{ab} + \kappa t_{ab} r_{bc} t_{ba} e^{i\phi} \quad (2)$$

where $\kappa = 1/(1 - r_{bc} r_{ba} e^{i\phi})$ and $\phi = 4\pi n_b d \cos\theta_b / \lambda$. r_{ab} and t_{ab} are the amplitude reflectivity and transmittance at an interface from a to b, respectively, and are obtained from Fresnel's law. The (power) reflectivity is obtained as $R = |r|^2$. Thus, the thin-film interference is converted to the interference in a Fabry–Perot interferometer, the interfaces of which are usually covered with metal or a multilayer coating. Typical examples calculated for the case are shown in Figures 1 and 2. It is clear that at low reflectivity, the modification of the formula on the reflectivity is negligibly small, while at high reflectivity, the reflection spectrum shows periodic dips, where Equation (1) is applied for the destructive interference, as in a Fabry–Perot interferometer.

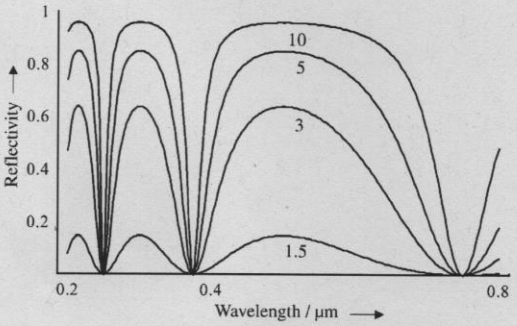

Figure 2. Reflectivity from a thin film of thickness 0.125 μm in air under normal incidence. The refractive index of the film is set to be 1.5, 3, 5, and 10.

2.2. Multilayer Interference

Multilayer interference is qualitatively understood as the case where a pair of thin layers piles up periodically. Consider two layers designated as A and B with thicknesses d_A and d_B and refractive indices n_A and n_B, respectively (Figure 3). We assume $n_A > n_B$ for the present. If we consider a particular pair of layers, the phases of the reflected light both at the upper and lower interfaces between B and A change by 180°. Thus, the relation of an antireflective coating, as in thin-film interference, can be applied as [Eq. (3)]:

$$2(n_A d_A \cos\theta_A + n_B d_B \cos\theta_B) = m\lambda \quad (3)$$

for constructive interference, with the angles of refraction in layers A and B as θ_A and θ_B, respectively.

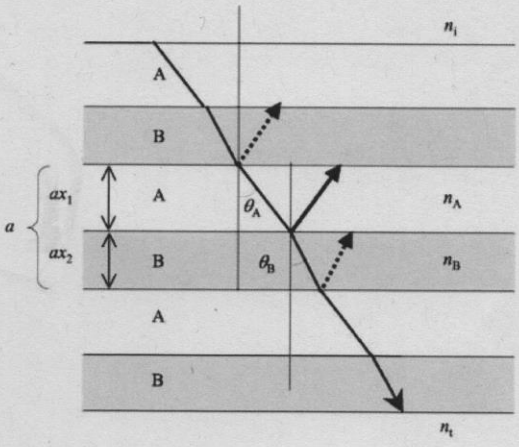

Figure 3. Configuration of the interference from a multilayer consisting of layers A and B with a thickness of ax_1 and ax_2 and a refractive index of n_A and n_B, respectively. n_i and n_t are the refractive indices of the incident and transmitting spaces. The dashed arrows indicate the reflected light subject to a phase change of 180°.

On the other hand, the phase of the reflected light does not change at an A–B interface. Thus, if a soap-bubble relation of Equation (1) [Eq. (4)]:

$$2n_A d_A \cos\theta_A = (m' + \frac{1}{2})\lambda \quad (4)$$

is further satisfied, the reflection from this interface adds to the above interference and the multilayer should give the maximum reflectivity, where $m' < m$ would be satisfied because of the restriction of the thickness. In particular, Equations (3) and (4) for $m = 1$ and $m' = 0$ correspond to the case where the optical path lengths, defined as the length multiplied by the refractive index, for layers A and B are equal to each other. Land called this case an "ideal multilayer".[14] However, if the thickness of layer A does not satisfy Equation (4), while the sum of layers A and B satisfies Equation (3), the reflection at the A–B interface works destructively and the peak reflectivity may decrease. This case corresponds to a "nonideal multilayer".

The calculation of the reflectivity from the multilayer has been fully described since Lord Rayleigh presented his paper in 1917.[5] Nowadays, the reflectivity and transmittance are usually calculated through a transfer matrix method. This method is suitable for the evaluation of structural colors, because it is applicable to multilayers having arbitrary refractive indices and thickness without any periodicity. Since the detail of the method has been described in the literature,[14–16] here we will show only the calculated results.

Figure 4a shows the reflectivity for an ideal multilayer with a varying number of layers under normal incidence. This figure corresponds to the cases where the difference in the refractive indices between the two layers is very small, which is a typical case for polymer materials. With increasing number of layers,

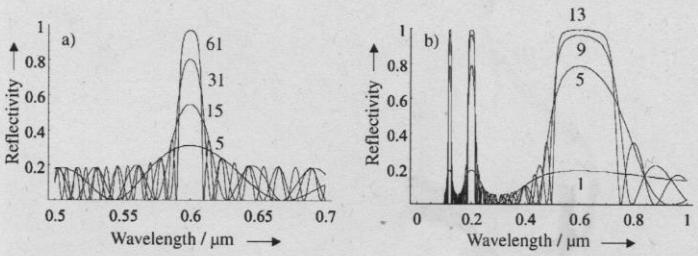

Figure 4. Reflectivity from a multilayer with various numbers of layers. a) The difference of the refractive indices for the two layers is small; $n_A = 1.55$ and $n_B = 1.60$. b) A large refractive index difference; $n_A = 1.6$ and $n_B = 1.0$. The thickness of each layer is set to satisfy an ideal multilayer and the total optical path length of the sum of layers A and B is set to 0.25 μm.

the reflectivity increases rapidly, while its bandwidth decreases remarkably. It is also noticed that an oscillation of the reflectivity of 0–20% is present in the background. This is because the difference between the refractive indices of air and the material is much larger than the interlayer difference. Thus, the multilayer behaves like a thin film.

Figure 4b shows the reflection spectrum of the multilayer with a large difference in the refractive indices of 0.6. When the difference of the refractive indices of the two layers becomes large, the maximum reflectivity reaches unity only with several layers. For an ideal multilayer under normal incidence, the maximum reflectivity occurs around the wavelengths where the relation $2n_Ad_A = 2n_Bd_B = (m+1/2)\lambda$ is satisfied. The amplitude reflectivity at this wavelength is calculated as $r = (1-p)/(1+p)$, where p satisfies the relations $p = (n_t/n_i)(n_B/n_A)^N$ and $p = (n_A^2/n_in_t)(n_A/n_B)^N$, in which the total number of layers N takes an even and odd number, respectively. Here we put the refractive indices of the incident and transmitting spaces as n_i and n_t. On the contrary, for the wavelength at which m is a half integer, the reflection from A–B and B–A interfaces interferes destructively. The reflectivity at this wavelength becomes $r = (n_i - n_t)/(n_i + n_t)$ and is null when the refractive indices of the incident and transmitting regions are the same. We can see this effect in Figure 4b, where the reflectivity at the wavelengths of 1/2, 1/4, 1/6, ... of the main wavelength becomes zero, while those of 1/3, 1/5, 1/7, ... form a peak.[14]

Next, we will briefly mention the result for a nonideal multilayer. Figures 5a and 5b show the calculated results corresponding to Figures 4a and 4b, in which the ratio of the optical path length of layer A with a higher refractive index decreases, while the sum of the optical path lengths is kept constant. Figure 5a shows the result for a small difference in the refractive indices. The peak reflectivity decreases with increasing asymmetry, while the bandwidth slightly decreases. At the same time, the peak position shifts toward shorter wavelengths. Figure 5b shows the result for a large difference in the refractive indices. The deviation from the ideal multilayer becomes remarkable, that is, both the peak reflectivity and the bandwidth decrease with increasing asymmetry. It is also noticed that the reflectivity at a wavelength of 1/2, 1/4, 1/6, ... of the main wavelength restores quickly.

Equations (3) and (4) are, however, too simple to express the essential features of the multilayer interference. In fact, they are only applicable to the case where the difference in the refractive indices of the two layers is sufficiently small. Otherwise, the multiple reflections modify the interference condition to a large extent. Details on this point are discussed in conjunction with recent studies on photonic crystals. Namely, the system with an infinite number of layers is the simplest case of a one-dimensional photonic crystal, in which the dielectric constant is periodically modulated. Here, we will consider only the first reflection band, that is, $k \approx \pi/a$ and $\omega \approx b_0 k/\sqrt{\mu_0}$, with a and μ_0 the period of the multilayer and the permeability of the vacuum, respectively. b_j is the expansion coefficient of the reciprocal of the dielectric constant with respect to the reciprocal lattice vector and is given below. After complicated calculations, we finally obtain the approximate expression for the dispersion relation near the first bandgap as [Eq. (5)]:[17]

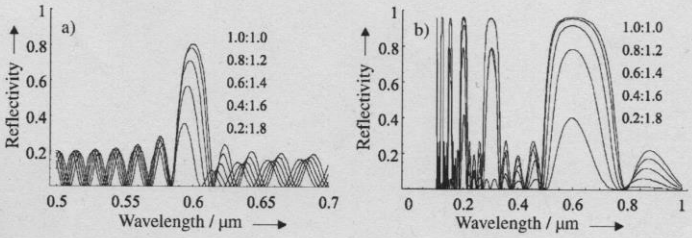

Figure 5. Reflectivity from a nonideal multilayer corresponding to Figure 4. a) A small difference in the refractive index and b) a large difference. The total optical path length is set to take a constant value of 0.25 μm, while the ratio of the optical path lengths for layers A and B is varied as indicated in the figure.

$$\omega_{\pm}(h) \approx \frac{\pi}{a\sqrt{\mu_0}}\sqrt{b_0 \pm |b_1|} + \frac{a}{2\pi\sqrt{\mu_0}\sqrt{b_0 \pm |b_1|}}\left(b_0 \pm \frac{2b_0^2 - |b_1|^2}{|b_1|}\right)h^2 \quad (5)$$

where $h \equiv k - \pi/a$. A schematic diagram for the dispersion relation of a one-dimensional photonic crystal is shown in Fig-

ure 6a. The bandgap just corresponds to the high-reflection band, whose band center and bandwidth correspond to $\omega_c = \pi\sqrt{b_0 \pm |b_1|}/(a\sqrt{\mu_0})$ and $\Delta\omega = \omega_+ - \omega_-$, respectively. For

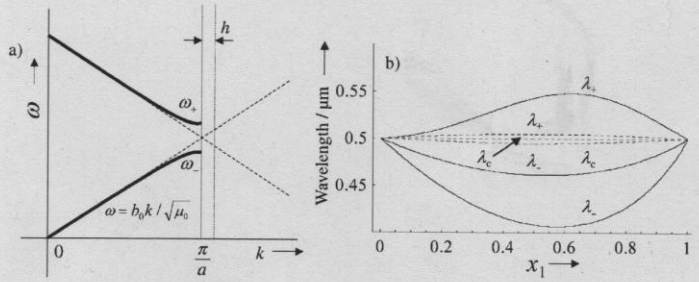

Figure 6. a) Schematic illustration of the dispersion curve near the first bandgap and b) upper and lower edges of a one-dimensional photonic bandgap for the small difference in the dielectric constant of $\varepsilon_1 = 1.55^2$ and $\varepsilon_2 = 1.60^2$ (-----), and for the large difference of $\varepsilon_1 = 1.60^2$ and $\varepsilon_2 = 1.00^2$ (——). The optical path length of the sum of the two layers is 0.25 μm.

periodic double layers whose dielectric constants are expressed as $\varepsilon_1 = n_1^2$ and $\varepsilon_2 = n_2^2$, the band center in a wavelength unit λ_c is expressed as Equation (6):

$$\lambda_c = 2a/\sqrt{\frac{1}{n_2^2}\left\{1 + \frac{n_2^2 - n_1^2}{n_1^2}x_1\right\}} \qquad (6)$$

where we put $b_0 = (x_1/n_1^2) + (x_2/n_2^2)$ and $|b_1| = \sin(\pi x_1)(n_1^{-2} - n_2^{-2})/\pi$ with x_1 and x_2 as the ratios of the thickness of the layers 1 and 2 to their sum. When $n_1 \approx n_2$, this reduces to $\lambda_c \approx 2a(n_1x_1 + n_2x_2)$, which corresponds to Equation (3). Figure 6b shows the calculated results of λ_c and $\lambda_\pm$ ($\equiv 2\pi/\omega_\mp(0)$) for small and large differences in the refractive indices between the two layers. It is clear that the bandwidth in the large difference in the refractive index is much larger than that in the small difference. Moreover, it is found that the deviation of the band center from Equation (3) becomes remarkable. In the following sections, the reader will soon understand that the fundamental optical processes, such as interference, diffraction, and scattering of light, are complicatedly connected with various structures to generate unique structural colors in nature.

3. Structural Colors in *Morpho* Butterflies

3.1. Historical Review

Morpho butterflies bearing brilliant blue color in their wings are the most suitable creatures to explain the complicated features of the structural colors in nature, and also to understand the importance of the regularity and irregularity in their colors. *Morpho* species live exclusively in Central and South America, and their males are especially brilliant. We show typical examples in Figure 7. So far, 50–80 species are classified into genus *Morpho*, although the systematic classification is still in progress.[18]

About 120 years ago, Walter[3,6] reported the observation of the scales of *M. menelaus*, which strongly glittered green-blue in air, became purely green and shining less strongly in ether ($n = 1.36$), yellowish green and weakly shining in chloroform ($n = 1.45$), and only perceptibly yellow-green under direct sunshine in a dark room when immersed in benzene ($n = 1.52$) or carbon disulfide ($n = 1.64$). Walter ascribed this phenomenon to the effect of dyes in chitin, whose refractive index is coincident with that of benzene or carbon disulfide. Michelson[4] measured the phase change in the reflection from the blue wing of *M. aega* under normal incidence and found that it changed with the orientation of the wing. He attributed this change to the diffraction of light by many hairs growing on the wing, and concluded that the essential cause of the blue color was the "surface color".

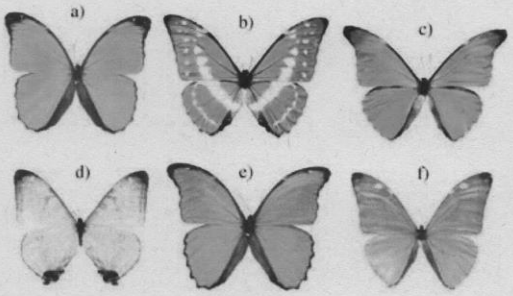

Figure 7. *Morpho* butterflies. a) *M. menelaus* (wingspan = 110 mm), b) *M. cypris* (120 mm), c) *M. rhetenor* (120 mm), d) *M. sulkowskyi* (85 mm), e) *M. didius* (155 mm), and f) *M. adonis* (95 mm) [photographed by Okamoto].

Lord Rayleigh,[5,6] on the other hand, strongly suggested the possibility of multilayer interference in brilliant colors. Onslow[8] investigated the scales of *M. menelaus* and found that two layers of scales were combined to form the brilliant greenish blue. The lower scale had periodic chitin plates 0.85–0.9 μm apart, each of which was transparent and prolonged as compared with the noniridescent scale. However, the separation of the plates he observed was too long to ascribe it to any interference phenomenon. More thorough investigation was made by Mason,[12] who investigated the scales of *M. menelaus* and found that the scale was constituted by many vanes and that a single vane itself was responsible for the brilliant reflection. He also found that the reflected plane was not parallel to the plane of the scale. He compared the optical properties with thin-layer interference and found a resemblance. In his paper,

